

Supporting Information

CO₂ Electroreduction to Formate - Comparative Study regarding the Electrocatalytic Performance of SnO₂ Nanoparticles

Henning Weinrich¹, Bastian Rutjens^{1,2}, Shibabrata Basak¹, Bernhard Schmid¹, Osmane Camara¹,
Ansgar Kretzschmar¹, Hans Kungl¹, Hermann Tempel¹ and Rüdiger-A. Eichel^{1,2,*}

¹ Institute of Energy and Climate Research–Fundamental Electrochemistry (IEK-9),
Forschungszentrum Jülich GmbH, 52428 Jülich, Germany

² Institute of Physical Chemistry, RWTH Aachen University, Landoltweg 2,
52074 Aachen, Germany

* Correspondence: r.eichel@fz-juelich.de

Materials and Methods

Materials

All electrolytes and eluents were prepared from fully deionized water (18.2 M Ω -cm, PURE-LAB flex 3, Elga Veolia, United Kingdom). As an electrolyte, 0.1 M KHCO₃ was prepared from commercially obtained KHCO₃ (≥ 99.7 %, Honeywell, Germany) and used without further purification.

Catalysts

SnO₂ (Commercial)

Commercial SnO₂ nanopowder was obtained from Sigma Aldrich (≤ 100 nm, LOT: MKCD 7402) and used without further purification.

SnO₂ (Hydrothermal)

SnO₂ (Hydrothermal) was prepared according to a method.¹ For the preparation in three separate batches, SnCl₄ · 5 H₂O (1.065 g, 1.063 g and 1.061 g, approx. 3 mmol, ≥ 98.0 %, Acros Organics, Germany) was dissolved in deionized water (60 mL, approx. 3.33 mol). Ethylenediamine (0.8 mL, approx. 12 mmol, ≤ 100 %, Merck, Germany) was added dropwise and stirred for 5 min in a Teflon-lined autoclave. The autoclave was heated and held at 180 °C for about 24 h in an oven. After cooling at ambient conditions, the resulting products were washed with deionized water, centrifuged, united and dried under vacuum at 60 °C. The product was obtained as a plain white powder. Yield: 1.107 g (81%).

SnO₂ (Solid-State)

SnO₂ (Solid-State) was prepared according to a two-step method.² In a typical synthesis SnCl₂ · 2 H₂O (2.560 g, approx. 11 mmol, ≥ 98.0 %, VWR Chemicals, Germany) and KOH (1.290 g,

approx. 23 mmol, EMSURE ACS, ISO, Reag. Ph. Eur., Merck, Germany) were manually ground for 30 min. The resulting brown powder was mixed with deionized water, sonicated in an ultrasonic bath, and centrifuged several times until the decanted water was free of chloride ions (0.1 M silver nitrate solution). The powder was dried and calcined at 600 °C for 2 h in a tube furnace under compressed air. The product was obtained as a gray powder. Yield: 0.922 g (53%).

SnO₂ (Sol-Gel)

The preparation of SnO₂ (Sol-Gel) was performed according to a sol-gel method.³ In a typical synthesis SnCl₂ · 2 H₂O (7.681 g, approx. 34 mmol, 98.0%+, VWR Chemicals, Germany) was dissolved in absolute ethanol (28 mL, approx. 0.48 mol, ≥99.8 %, Honeywell, Germany). 0.9 mL HCl were added to adjust the pH between 2 and 3. The acidic solution was stirred for 24 h. During this time, first, the solution became transparent and turned into a white gel later. 175 mL deionized water were added, and the gel turned yellow. After additional 24 h stirring the solvent was evaporated and the resulting tin gel was calcined at 600 °C for 2 h in a tube furnace under compressed air. The product was obtained as a light-gray powder. Yield: 2.053 g (40%).

Material Characterization

The analysis of the crystal structure was carried out using powder X-ray diffraction (XRD)-measurements with an EMPYREAN (Panalytical, The Netherlands) X-ray diffractometer with Cu–K α radiation, operating at 40 kV, 40 mA and a scan rate of about 1°·min⁻¹.

Raman spectra were obtained using a Senterra Raman microscope (Bruker, USA) at ambient conditions. The excitation wavelength was 532 nm with a power of 20 mW. The signals of two subsequent measurements of 5 s at one spot were added up, to improve the signal to noise ratio of a single measurement (co-addition mode). Furthermore, the spectra of several spots were merged and normalized upon analysis, providing a general spectrum for each sample.

The BET-results were obtained using a 3P micro 300C (3P Instruments, Germany) for N₂-physisorption at 77 K (5 N, Air Liquid, France). Prior to every BET measurement all samples were evacuated for at least 48 h at 60 °C, attaining reproducible experimental conditions for the gas adsorption measurements.

The SEM-images were acquired on a Quanta FEG 650 ESEM (FEI, Germany) at a typical acceleration voltage of 20 kV and a working distance of 10 mm. For the TEM-characterization, the SnO₂ particles were drop casted onto typical TEM-grids. The bright field images, selected area electron diffraction patterns and high-resolution images were obtained using a FEI Tecnai operating at 200 kV. The energy dispersive X-ray maps were obtained using a FEI Titan G2 80-200 Chemi STEM equipped with a Super-X EDX system operating at 80 kV.

Electrode Preparation

For the investigation of the catalysts, 5 mg·mL⁻¹ of the individual materials were dispersed in a 3:1 mixture of deionized water and isopropanol (≥99.7%, VWR Chemicals, Germany), adding 1.75 Vol.% of a NafionTM dispersion as a binder (5 wt.% in lower aliphatic alcohols and water, Sigma-Aldrich, Germany). This mixture was ultrasonicated in an ultrasonic bath for a minimum of one hour to guarantee homogeneity of the resulting catalyst ink. Furthermore, the ink was re-dispersed prior to every electrode preparation using an ultrasonic probe. Afterwards, the ink was deposited onto a freshly polished glassy carbon substrate applying 20 µL at a surface area of 0.196 cm² (catalyst loading = 0.51 mg/cm²). The resulting electrode was dried at ambient conditions until the catalyst film consolidated completely.

Electrode Characterization

The electrode characterization was performed using a rotating disc electrode (RDE)-setup, which is schematically depicted in Figure S1. The setup consisted of a Modulated Speed Rotator (Pine Research Instruments, USA) with a 15 mm PEEK shaft that accepts *ChangeDisk* RDE tips holding 5 mm interchangeable discs. The reaction vessel was a custom-made H-type glass cell with two compartments, which were separated by a NafionTM 117 cation exchange membrane (Ion Power Store, Germany). The electrolyte volume for each of the two compartments was approx. 75 ml, which were filled with 60 mL of 0.1 M KHCO₃ each. One compartment hosted the RDE as the working electrode (WE), the reference electrode (RE, Ag/AgCl (3M KCl), ALS, Japan) and a CO₂ purge nozzle with a glass frit. The RE was attached to the glass cell and positioned in close proximity to the WE via a Luggin capillary. The other compartment hosted the counter electrode (CE), which was a twined platinum wire. 10 min prior, as well as during the experiment, the electrolyte in the RDE half-cell compartment was (constantly) purged with CO₂ (4.5N, Air Products, Germany), to reach and maintain a constant CO₂ concentration in the electrolyte. Furthermore, during every experiment, the RDE was rotated with a rotational speed of 2000 rpm.

The electrochemical experiments were carried out on a SP-200 potentiostat (BioLogic, France) according to the following procedure, using a fresh electrode for each run: First a linear cathodic potential sweep was conducted from the open circuit potential (OCP) to the desired electroreduction potential followed by 3 h of potentiostatic electroreduction. The potential lay in a range from -1.2 V to -2.0 V vs. Ag/AgCl. After the experiment, another linear potential sweep was conducted from -1.0 V vs. Ag/AgCl to the previous electroreduction potential to investigate potential changes of the catalyst in the same electrolyte. During the ongoing reaction, four 1 mL electrolyte

samples were collected after 0.25, 1, 2 and 3 h for product analysis by ion chromatography without refill.

All potentials within this paper are reported with reference to the Reversible Hydrogen Electrode (RHE), recalculating the potential of the RE according to the following equation and assuming a constant pH of the CO₂ saturated electrolyte (0.1 M KHCO₃) of pH = 6.81.

$$E(\text{RHE}) = E(\text{Ag/AgCl}) + 0.059 \text{ V} \cdot \text{pH} + 0.210 \text{ V} \quad (\text{S1})$$

Each potential reported in this study represents the cathode potential of the RDE-tip vs. the reference electrode. The anode potential has not been recorded given the vast overpotential between the reference electrode in the RDE half-cell and the counter electrode.

Quantification of Formate

The amount of formate produced during the CO₂ electroreduction were determined via ion exclusion chromatography (IEC), using an S155 ion chromatograph (Sykam Ionenchromatographie Vertriebsgesellschaft mbH, Germany) equipped with an autosampler and a SykroGel-Ex 450SA-E01 column. The eluent was a 0.7 mM solution of heptafluorobutyric acid (99%, Acros Organics, Germany) in a 7 vol.-% solution of acetonitrile (isocratic grade for liquid chromatography, Supelco, Germany) in water. Analytes were detected with a conductivity cell after chemical suppression with 50 mM LiOH. The quantification error for the determination of formate of 5-20% is given based on conservative estimates depending on the observed amount/concentration of formate. The lower detection limit of the ion chromatograph for formate is 10⁻⁶ mol/L. In this study, the following error intervals were considered:

$$c < 3.33 \cdot 10^{-5} \text{ mol/L} - 20\%$$

$$c < 10^{-4} \text{ mol/L} - 10\%$$

$c > 10^{-4} \text{ mol/L} - 5\%$

COMPARISON WITH CORRESPONDING LITERATURE

The synthesis methods, used for the preparation of the SnO₂ nanoparticles investigated in this study have been extracted from literature.¹⁻³ Comparing the present results with their individual counterparts, commonalities and differences can be found.

The syntheses of SnO₂ nanoparticles by the hydrothermal method in literature resulted in a phase pure, white powder, which was, among other methods, further investigated by TEM, SAED and Raman spectroscopy.¹ In the TEM analysis, the most frequently found particle size fraction was 3.5 to 4.0 nm, while the XRD analysis provided an average grain size of 3.6 nm. Furthermore, based on SAED, it was concluded that the investigated particles were polycrystalline, predominantly showing Raman bands at 572, 631, 476 and 431 cm⁻¹ with a clear emphasize on 572 and 631 cm⁻¹. Comparing these results with the results of the present study it can be concluded that the synthesis of SnO₂ by the hydrothermal method was reproduced successfully. The nanoparticles of the plain white catalyst powder investigated in this study feature about the same grain size of 3.1 nm based on XRD, show a similar particle size of about 5 nm based on TEM and exhibit a very similar Raman spectrum with a very similar relation for the two Raman bands at 572 cm⁻¹ and 631 cm⁻¹. However, polycrystallinity could not be observed in the present investigation, as the HRTEM images show single crystalline particles (cf. Figure 3).

Using the solid-state synthesis method, in literature a pale powder with particles of about 20 nm was obtained after calcination at 600 °C as determined by XRD and TEM.² During the synthesis, first, large SnO particles (~500 nm) were observed prior to calcination, but led to finer SnO₂ nanoparticles after calcination later, which was presumably due to a peel-off mechanism starting from the large SnO particles. In connection with the present observations, the lack of sufficient peel-off could be an explanation for the significant agglomeration of the SnO₂ (Solid-

State) nanoparticles, which was determined by the lack of BET surface area. Apart from that, the TEM particle size (>10 nm) and XRD grain size (26.6 nm) mostly match with the reference, while the resulting powder in the present study showed deviations from a typical white color, too. Thus, the solid-state synthesis was successfully reproduced.

Furthermore, looking at SnO_2 (Sol-Gel) in comparison to the results in literature³, it can be concluded that the third synthesis method was successfully reproduced as well. Again, the resulting particle sizes determined by TEM (10 to 20 nm), match with literature (~ 20 nm). Moreover, in both cases, the XRD patterns suggest phase pure SnO_2 material. However, since the original publication focused on battery applications, the options to compare both materials are limited, since a Raman-investigation has not been pursued and since the addition of graphite³ prevents the comparison of the catalyst color, which, judged by previous observations², appears to be a means to detect residual species different from SnO_2 , such as SnO , by eye.

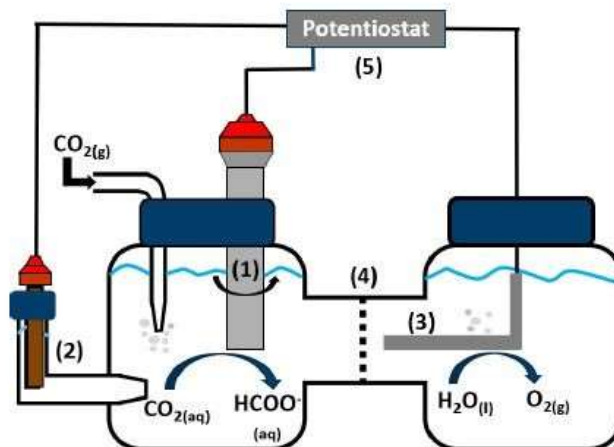


Figure S1 - Schematic representation of the experimental setup used for the RDE experiments. (1) Shaft of the rotating disc electrode (RDE) including the RDE underneath (working electrode), (2) reference electrode, (3) Pt-counter electrode, (4) Nafion membrane, (5) potentiostat.

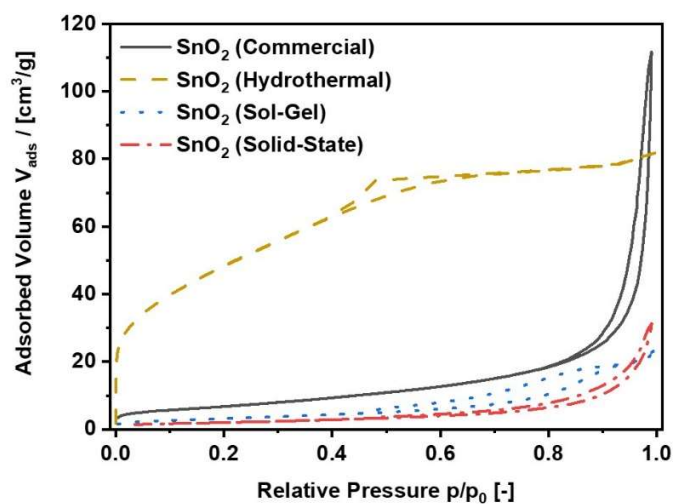


Figure S2 - N₂-sorption isotherms of the investigated SnO₂ nanoparticles.

CALCULATION OF BET-PARTICLE SIZE:

$$d = \frac{6}{S_{BET} \cdot \rho_{SnO_2}} \quad (S2)$$

Derivation of equation S1:

$$S_{BET} = \frac{A_{sphere}}{m_{sample}}$$

$$m_{sample} = \rho_{SnO_2} \cdot V_{sphere}$$

$$V_{sphere} = 1/6 \pi d^3$$

$$A_{sphere} = \pi d^2$$

d = particle diameter

S_{BET} = specific surface area determined by BET-analysis

ρ_{SnO_2} = density of SnO_2 (= $6.95 \text{ g}\cdot\text{cm}^{-3}$)

A_{sample} = surface area of the particular sample determined by BET-analysis

m_{sample} = weight of the particular sample analyzed by BET

V_{sphere} = volume of a sphere

A_{sphere} = surface area of a sphere

DEBYE-SCHERRER EQUATION:

$$L = \frac{K \cdot \lambda}{\Delta(2\theta) \cdot \cos(\theta)} \quad (\text{S3})$$

L = mean grain size

K = dimensionless shape factor (= 0.9)

λ = X-ray wavelength

$\Delta(2\theta)$ = full width of half maximum for [110]-reflex

θ = Bragg angle (= 26.7 °)

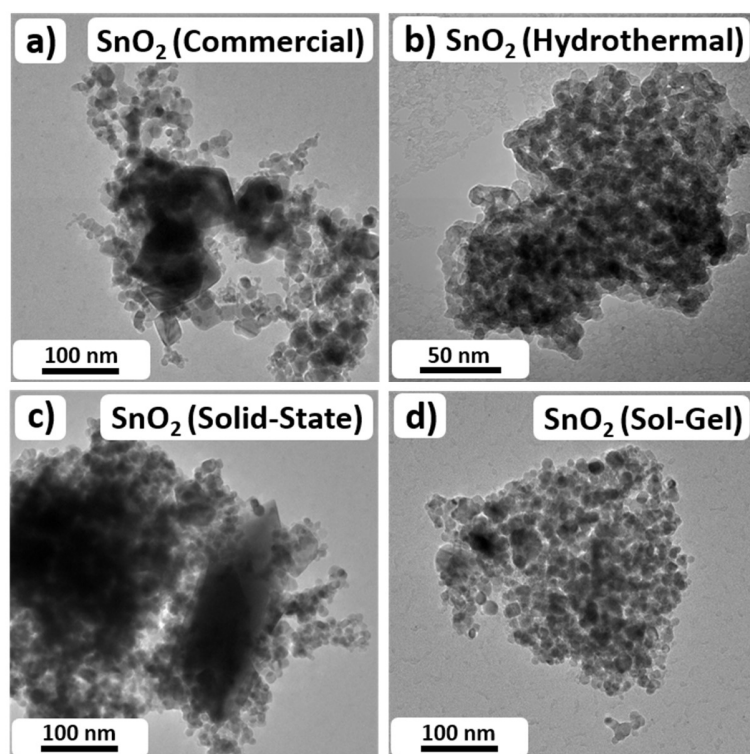


Figure S3 - TEM images of the investigated SnO_2 nanoparticles at low magnification. (a) SnO_2 (Commercial); (b) SnO_2 (Hydrothermal); (c) SnO_2 (Solid-State); (d) SnO_2 (Sol-Gel).

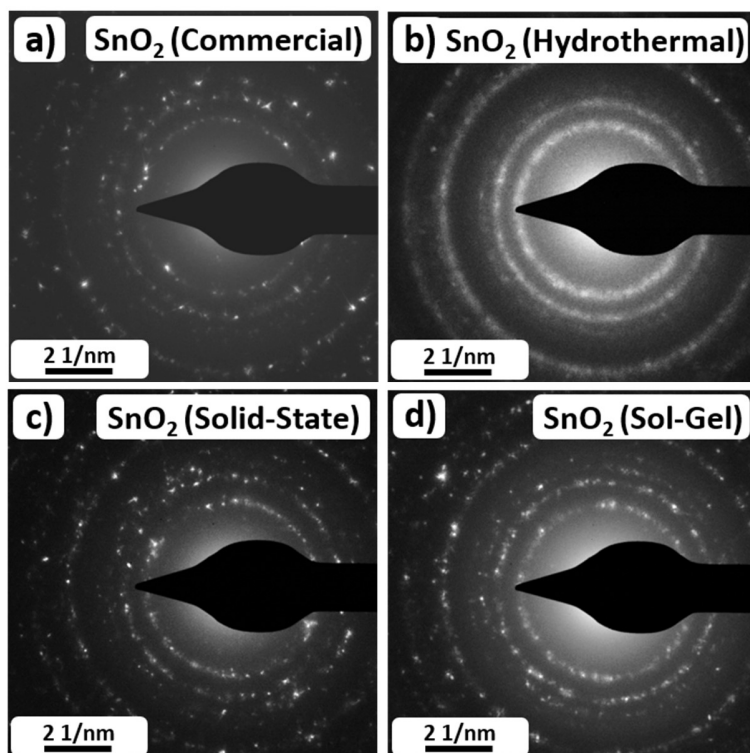


Figure S4 - Selected area diffraction pattern for the investigated SnO₂ catalyst. (a) SnO₂ (Commercial); (b) SnO₂ (Hydrothermal); (c) SnO₂ (Solid-State); (d) SnO₂ (Sol-Gel).

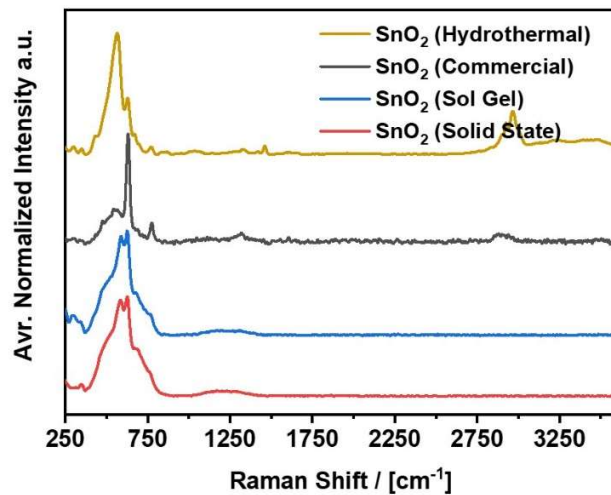


Figure S5 - Complete Raman spectra of the investigated SnO₂ nanoparticles.

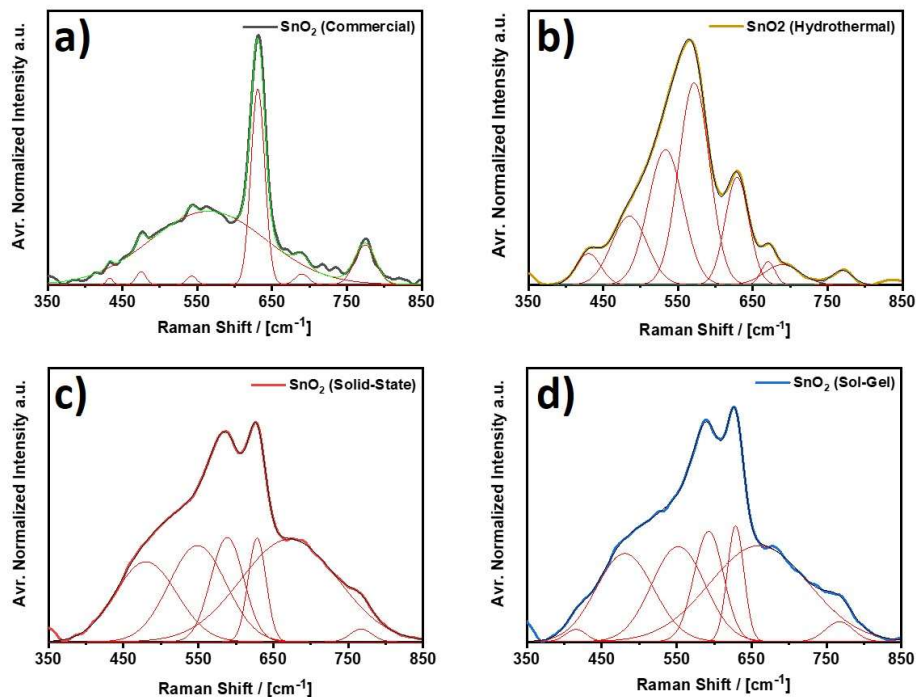


Figure S6 - Result of the peak deconvolution for the Raman spectra shown in Fig. 5. (a) SnO₂ (Commercial); (b) SnO₂ (Hydrothermal); (c) SnO₂ (Solid-State); (d) SnO₂ (Sol-Gel).

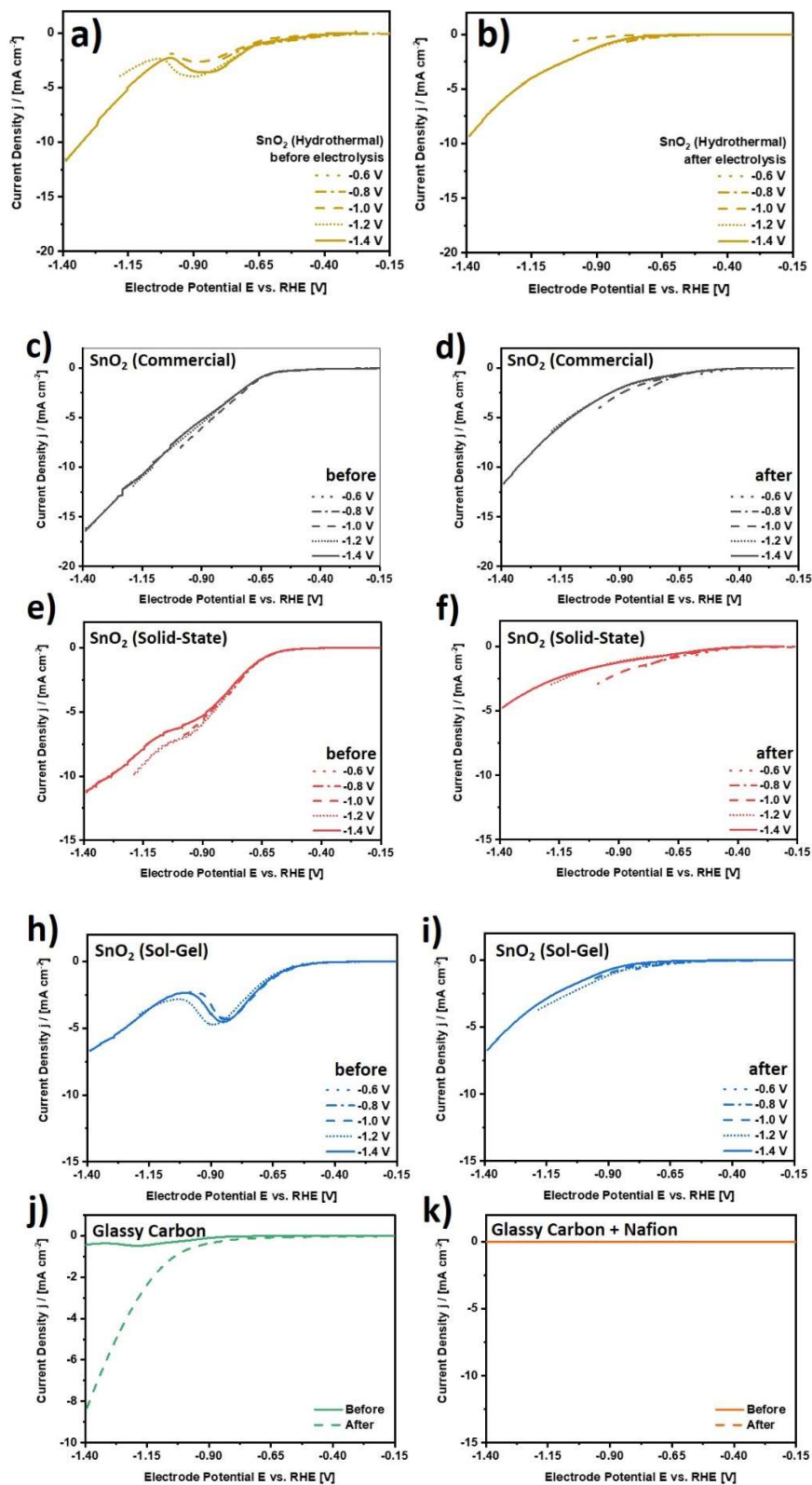


Figure S7 - LSV results for the investigated SnO₂ catalysts analogous to Fig. 6. (a,b) SnO₂ (Hydrothermal) before and after electrolysis; (c,d) SnO₂ (Commercial) before and after electrolysis; (e,f) SnO₂ (Solid-State) before and after electrolysis; (h,i) SnO₂ (Sol-Gel) before and after electrolysis; (j) Glassy Carbon (reference); (k) Glassy Carbon + Nafion (reference).

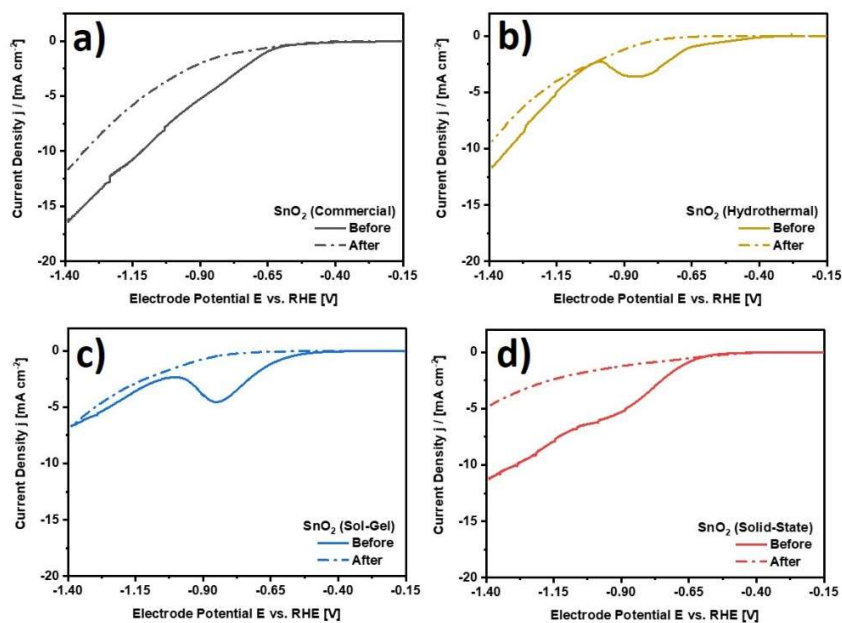


Figure S8 - Direct comparison of LSV scans to -1.4 V vs. RHE before and after three hours of CO₂-electrolysis for all investigated SnO₂ nanoparticles analogous to Fig. 6. (a) SnO₂ (Commercial); (b) SnO₂ (Hydrothermal); (c) SnO₂ (Solid-State); (d) SnO₂ (Sol-Gel).

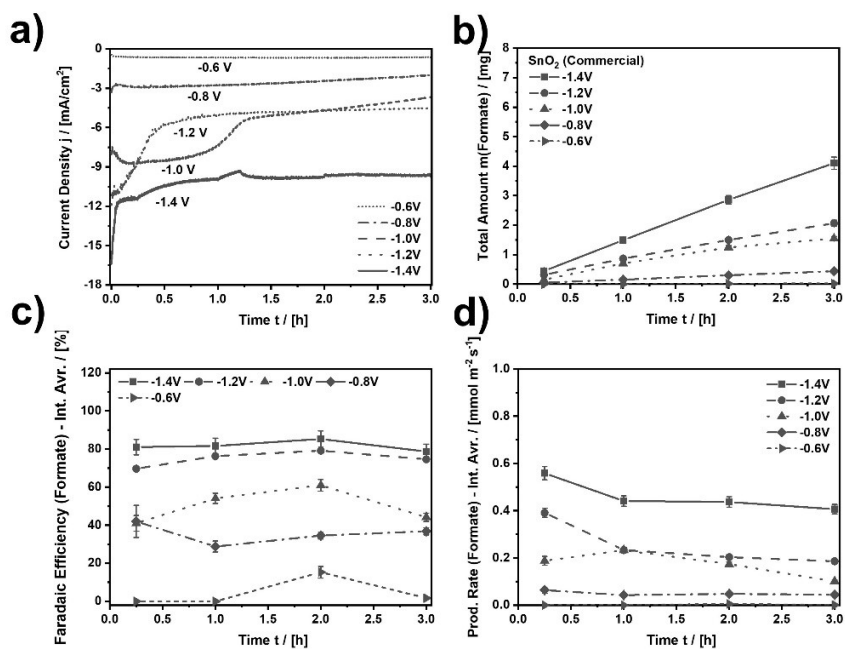


Figure S9 - Performance analysis of SnO₂ (Commercial) analogous to the results shown in Fig.7. (a) Applied current density (current normalized by RDE area, A = 0.196 cm²); (b) Total amount of formate produced by CO₂ electroreduction; (c) Faradaic efficiency for the CO₂ERR to formate (Interval averages: 0–0.25 h, 0.25–1 h, 1–2 h, and 2–3 h); (d) Production rate of formate (Interval averages: 0–0.25 h, 0.25–1 h, 1–2 h, and 2–3 h).

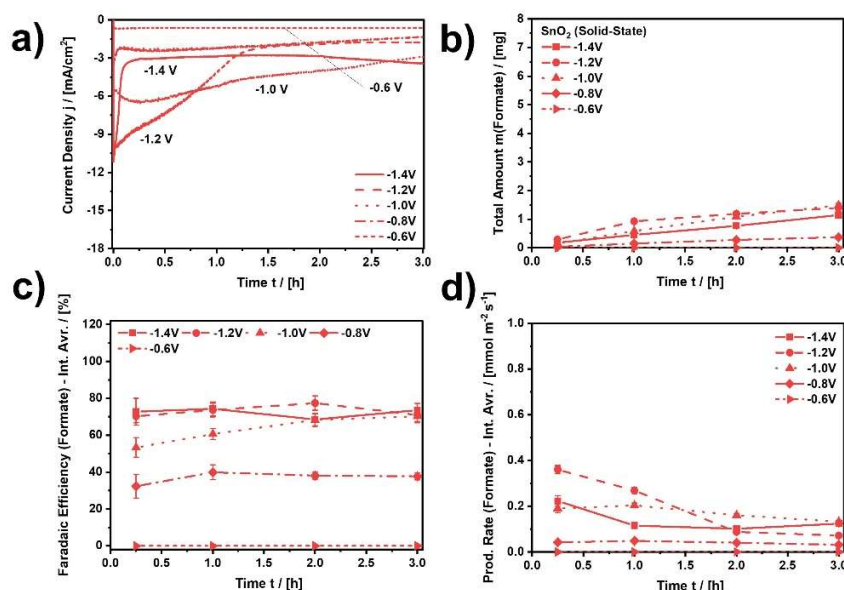


Figure S10 - Performance analysis of SnO₂ (Solid-State) analogous to the results shown in Fig.7. (a) Applied current density (current normalized by RDE area, $A = 0.196 \text{ cm}^2$); (b) Total amount of formate produced by CO₂ electroreduction; (c) Faradaic efficiency for the CO₂ERR to formate (Interval averages: 0–0.25 h, 0.25–1 h, 1–2 h, and 2–3 h); (d) Production rate of formate (Interval averages: 0–0.25 h, 0.25–1 h, 1–2 h, and 2–3 h).

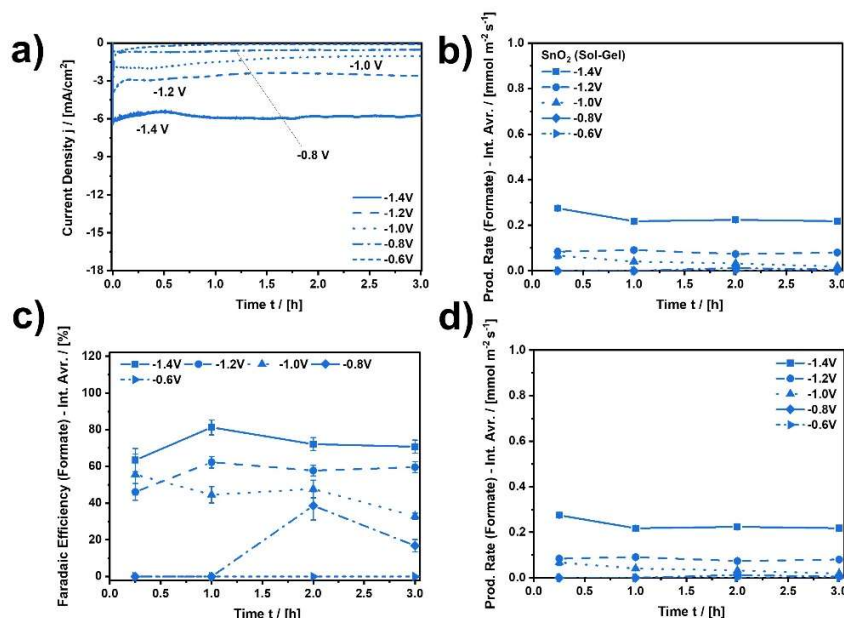


Figure S11 - Performance analysis of SnO₂ (Sol-Gel) analogous to the results shown in Fig.7. (a) Applied current density (current normalized by RDE area, $A = 0.196 \text{ cm}^2$); (b) Total amount of formate produced by CO₂ electroreduction; (c) Faradaic efficiency for the CO₂ERR to formate (Interval averages: 0–0.25 h, 0.25–1 h, 1–2 h, and 2–3 h); (d) Production rate of formate (Interval averages: 0–0.25 h, 0.25–1 h, 1–2 h, and 2–3 h).

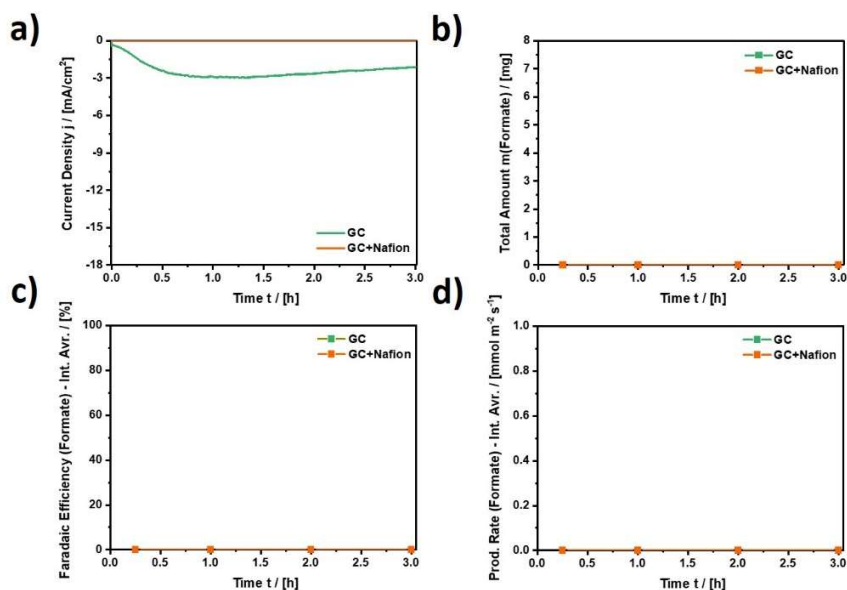


Figure S12 - Reference performance of glassy carbon and glassy carbon covered with Nafion at -1.4 V vs. RHE analogous to the results shown in Fig. 7. (a) Applied current density (current normalized by RDE area, $A = 0.196 \text{ cm}^2$); (b) Total amount of formate produced by CO₂ electroreduction; (c) Faradaic efficiency for the CO₂ERR to formate (Interval averages: 0–0.25 h, 0.25–1 h, 1–2 h, and 2–3 h); (d) Production rate of formate (Interval averages: 0–0.25 h, 0.25–1 h, 1–2 h, and 2–3 h).

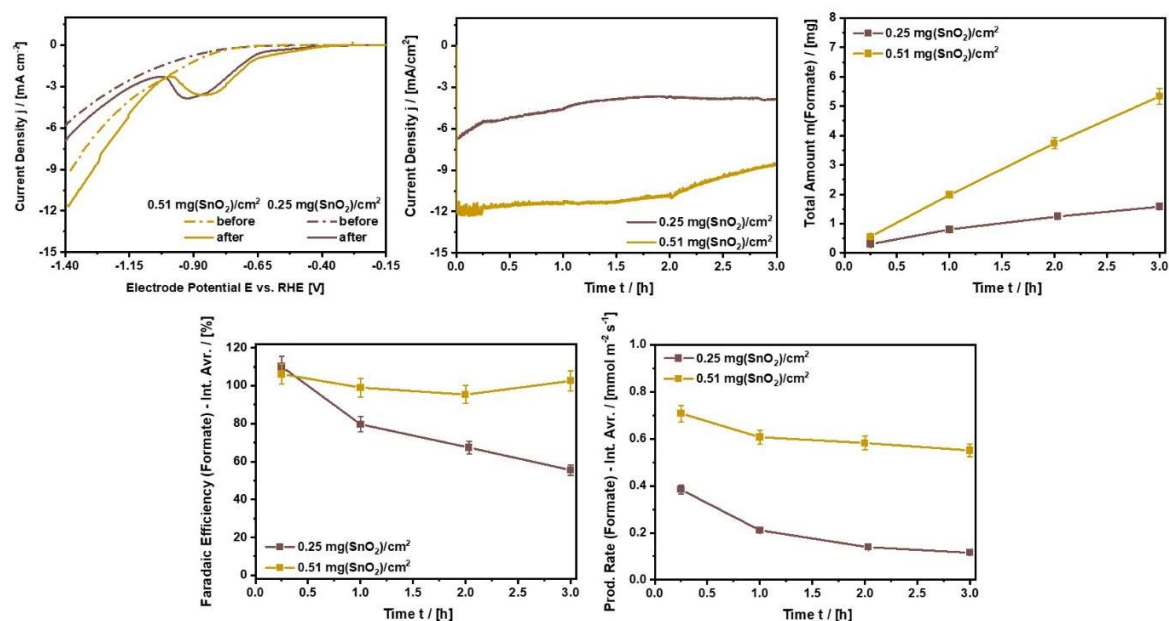


Figure S13 - Result of an additional reference experiment using half the amount of SnO_2 (Hydro-thermal) as compared to all the other experiments reported in this publication. CO_2 electrolysis performed at -1.4 V vs. RHE. Analysis analogous to Figs. 6-7.

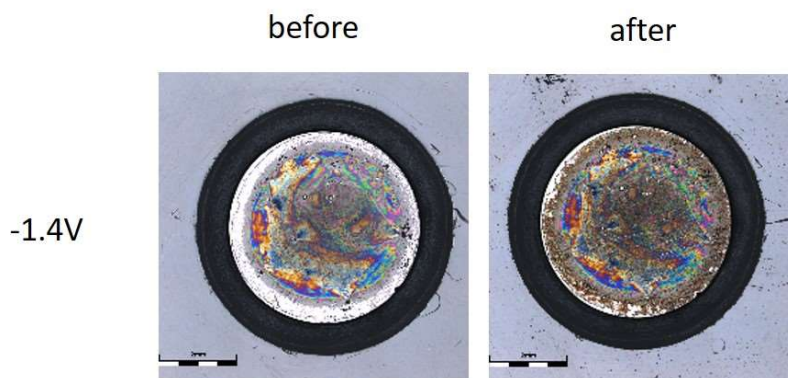


Figure S14 - Exemplary LSM images of the applied electrode bearing hydrothermal SnO_2 nanoparticles before and after electrolysis at -1.4 V vs. RHE in CO_2 -saturated and continuously purged 0.1M KHCO_3 at ambient conditions and 2000 rpm rotational speed of the RDE.

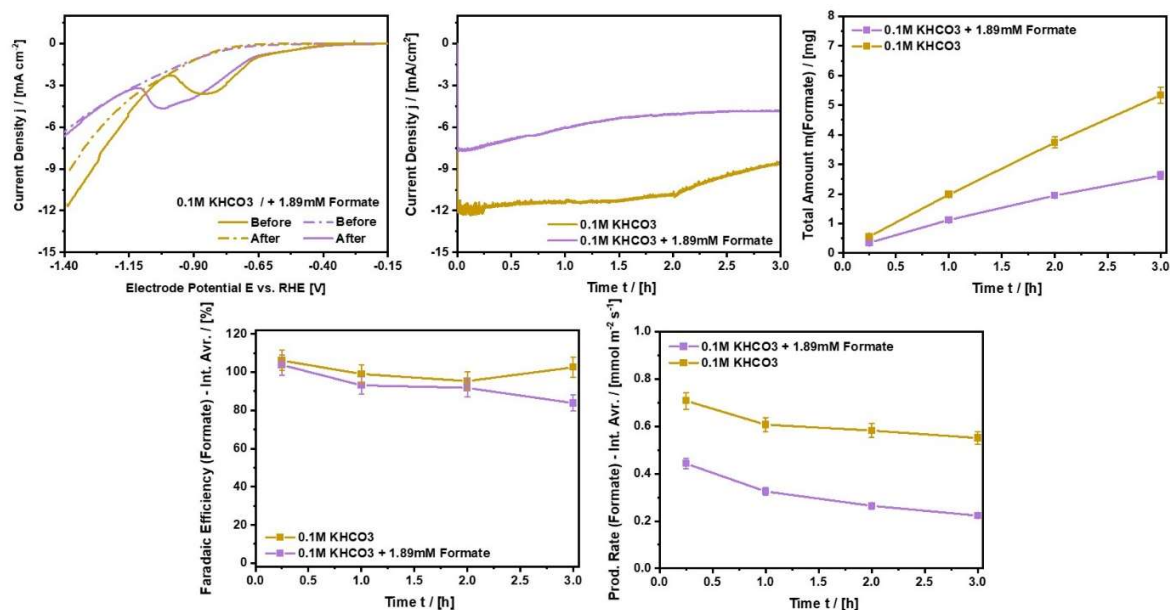


Figure S15 - Reference experiment showing the influence of formate on the performance of SnO₂ (Hydrothermal) at -1.4 V vs. RHE. For this experiment, 0.1M KHCO₃ containing 1.89 mM KHCO₂ was used as electrolyte and the experiment was performed analogously to the experiment shown in Figs. 6-7. (1.89 mM KHCO₂ \triangleq 5.1 mg in 60 mL [\triangleq final concentration for the experiment in the absence of formate (yellow)]).

REFERENCES

- (1) Liu, Y.; Yang, F.; Yang, X. Size-Controlled Synthesis and Characterization of Quantum-Size SnO₂ Nanocrystallites by a Solvothermal Route. *Colloids Surfaces A Physicochem. Eng. Asp.* **2008**, *312* (2–3), 219–225. <https://doi.org/10.1016/j.colsurfa.2007.06.054>.
- (2) Li, F.; Chen, L.; Chen, Z.; Xu, J.; Zhu, J.; Xin, X. Two-Step Solid-State Synthesis of Tin Oxide and Its Gas-Sensing Property. *Mater. Chem. Phys.* **2002**, *73* (2–3), 335–338. [https://doi.org/10.1016/S0254-0584\(01\)00357-1](https://doi.org/10.1016/S0254-0584(01)00357-1).
- (3) Chen, Y. C.; Chen, J. M.; Huang, Y. H.; Lee, Y. R.; Shih, H. C. Size Effect of Tin Oxide Nanoparticles on High Capacity Lithium Battery Anode Materials. *Surf. Coatings Technol.* **2007**, *202* (4–7), 1313–1318. <https://doi.org/10.1016/j.surfcoat.2007.08.048>.